Electron Transport Layer

Subjects: Materials Science, Coatings & Films

Contributor: Ying Chen

The electron transport layer (ETL) acts as a function of collecting electrons and blocking the transport of holes to the FTO electrode in the PSC. The mesoporous structure of the ETL promotes the crystallization and film formation of perovskite and shortens the migration path of photogenerated electrons. A suitable ETL should have an energy band position that matches the perovskite material.

perovskite solar cells | electron transport layer | perovskite preparation

1. Introduction

The serious consumption of energy and environmental problems have aroused people's attention to renewable energy. Over the past decade, solar energy systems have proved to be the most compelling of all renewable energy systems [1]. Perovskite is considered a hopeful photovoltaic candidate due to its high optical absorption coefficient, tunable band gaps, long charge carrier life, low cost, and simple preparation process [2][3][4][5][6][7]. The power conversion efficiency (PCE) of perovskite solar cells (PSCs) has jumped from 3.8% to 25.73% (certified) [8]. As shown in **Figure 1**, ABX_3 is the general formula crystal structure of perovskite materials. A is a large radius cation such as $CH_3NH_3^+$ (MA^+), $NH_2CH{=}NH_2^+$ (FA^+), Cs^+, Ca^{2+}, and Sr^{2+} B is Pb^{2+}, Sn^{2+}, Ti^{4+}, Nb^{5+}, Mn^{4+}, and other small radius cations. X are anions such as O_2, F^-, Cl^-, Br^-, and I^- [9][10]. The tolerance factor t could be used to calculate the perovskite crystal structure stability. The $t = (R_A + R_X)/2{-}\sqrt{2}(R_B + R_X)$, where R_A, R_B, and R_X refer to the ionic radii of A, B, and X site ions, separately. In general, the tolerance factor of structurally stable, highly symmetrical cubic structured perovskites usually ranges from 0.813 to 1.107 [11][12]. Within this range of tolerance factors, different stabilities and band structures of perovskite materials were obtained by doping or replacing the A, B, and X site ions [13]. For example, adding Sn to Pb-based perovskites could reduce the band gap and effectively broaden the absorption spectrum in the near-infrared [14][15]. With this advantage, perovskite materials can be combined with different forbidden bandwidths of light-absorbing materials, such as Si and quantum dots, to make stacked cells, such as perovskite-Si [16][17], perovskite-chalcogenides [18][19], and perovskite-quantum dots [20].

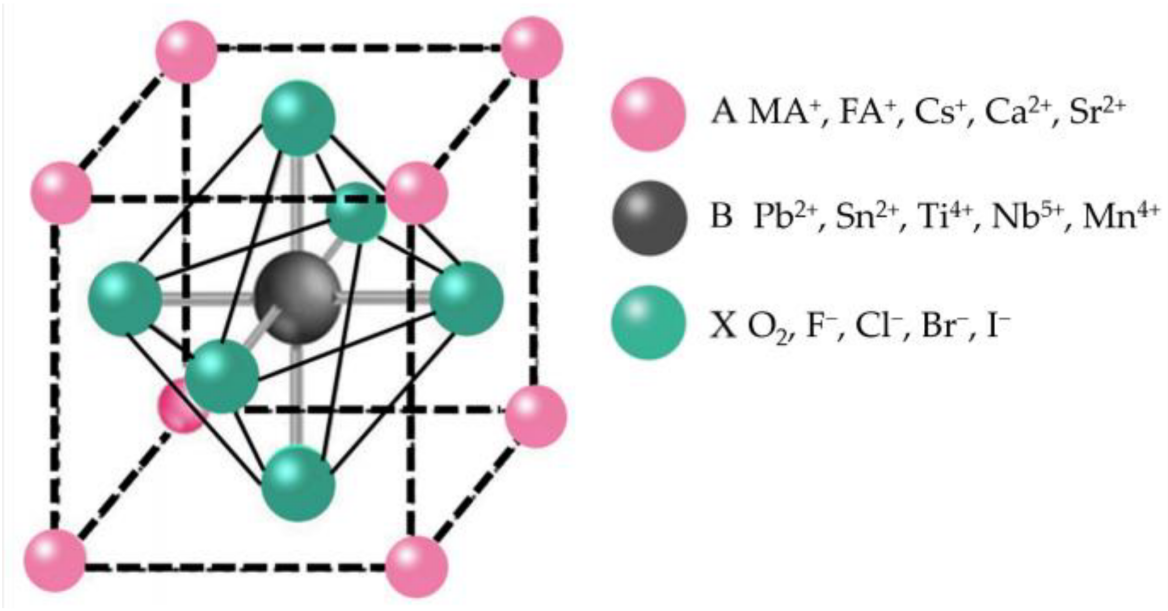

Figure 1. Typical crystalline structure of perovskite.

Perovskite solar cells are primarily divided into mesoporous structures and planar structures. The planar structures contain regular planar structures (n-i-p) and inverted planar structures (p-i-n) [21]. The typical mesoporous structures from bottom to top are a transparent conductive glass substrate (FTO, ITO), an electron transport layer (ETL), a mesoporous layer (mainly TiO_2, Al_2O_3, etc.), a perovskite layer, a hole transport layer (HTL), and metal electrodes (**Figure 2**a). The ETL plays the role of electron transport and hole blocking. The mesoporous layer is relatively thin. Thus, a perovskite layer could cover it completely to isolate the mesoporous material from HTL [22]. The HTL plays the role of hole transport. This structure avoids interfacial compounding of charges while maximizing charge transfer efficiency, enhancing the open-circuit voltage and charge collection efficiency, and most of the higher-certified efficiency perovskite solar cells use this structure [23]. However, the preparation of the mesoporous layers requires high-temperature processing, which limits its application in flexible devices.

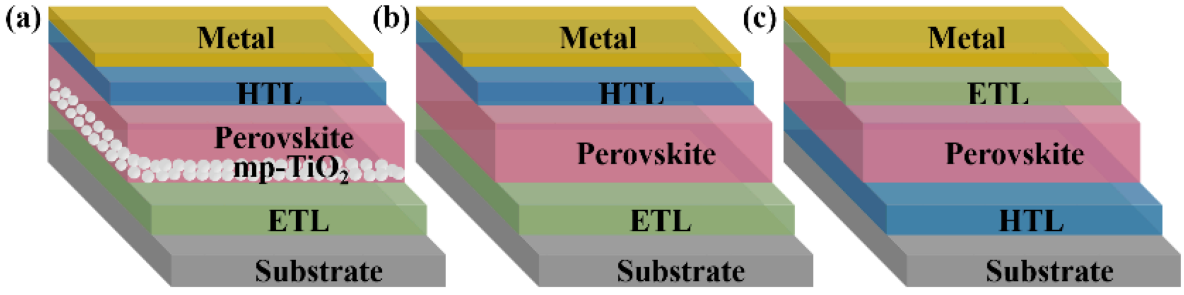

Figure 2. Three representative structures of PSCs: (**a**) mesoporous structures; (**b**) regular planar (n-i-p) structures, and (**c**) inverted planar (p-i-n) structures.

The planar structure is similar to a “sandwich structure”. The perovskite layer is placed between the n-type material and the p-type material, which benefits from the excellent bipolar carrier transport properties of perovskite

materials. They have n-i-p and p-i-n types (**Figure 2**b,c). The n-i-p structure is simplified from the mesoporous structure. The p-i-n structure is developed mainly from the structure and materials of classical organic solar cells. Planar-structured perovskite solar cells do not have a mesoporous layer, which is suitable for the fabrication of large-area flexible devices at low temperatures. Their preparation process is relatively simple too. However, without mesoporous material as a backbone, the perovskite morphology is difficult to control, the repeatability of the devices is poor, and additional auxiliary means are required to improve the film quality.

2. Electron Transport Layer (ETL)

The ETL acts as a function of collecting electrons and blocking the transport of holes to the FTO electrode in the PSC. The mesoporous structure of the ETL promotes the crystallization and film formation of perovskite and shortens the migration path of photogenerated electrons. A suitable ETL should have an energy band position that matches the perovskite material. The conduction band position should be slightly below the conduction band minimum of the perovskite layer to facilitate electron injection, while the valence band is at a deeper position to effectively block holes and has a high electron conductivity to ensure electron transport and collection [24].

TiO_2, an N-type oxide, is considered the most common choice for ETL material, with a wide band gap (~3 eV), easy-to-tune electronic properties, ability to form both dense and mesoporous layers, and producible easily and at low cost. TiO_2 has two thermodynamically stable crystal phases: anatase and rutile. Kim et al. [25] found that the anatase phase showed better performance than the rutile phase. However, Wang et al. [26] showed that a rutile TiO_2 ETL had better conductivity and match with the $MAPbI_3$ layer, which significantly enhanced performance. Several new methods to prepare TiO_2 for flexible devices or mass production have emerged in recent years, such as ball milling [27], ultrasonic spray [28][29], atomic layer deposition [30], inkjet-print [31][32][33], hydrothermal [34][35][36], sol–gel chemistry [37], low-temperature CO_2 plasma [38], and low-temperature microwave [39][40]. The morphology of TiO_2 has also attracted much attention. $TiCl_4$ was a good choice. Jarwal et al. [41] obtained TiO_2 nanorod arrays by solvothermal etching and/or $TiCl_4$ treatment to improve their surface-to-volume ratio and direct carrier transportation. Shahvaranfard et al. [42] adopted $TiCl_4$ treatment and a $PC_{61}BM$ monolayer to obtain a TiO_2 nanorod array ETL. Lu et al. [43] exquisitely tuned $TiCl_4$ precursor solution to construct nanowire arrays and nanoflower composite of TiO_2 film. The composite structure has the characteristics of a short direct charge transmission path, small leakage current and charge transmission resistance, slow recombination rate, and large light harvest. The best PCE was more than 20%. Doping is a great method for improving the quality of TiO_2. The commonly doped materials include Li [44], Mg [45], Zn [46][47], $EuAc_3$ [48], Nb [49], Ce [50][51], Zr [52][53], Ta [54][55], and graphene quantum dots (QDs) [56]. The performance of related PSCs is shown in **Table 1**. Bilayer ETLs also work well, such as TiO_2/SnO_2 [57][58][59][60][61][62][63][64][65][66], TiO_2/ZnO [67][68], TiO_2/WO_3 [69][70], TiO_2/graphene [71][72], TiO_2/fullerene [73], and TiO_2/NiO [74].

SnO_2, as an ETL material, has excellent electrical and optical properties. Its disadvantage is that there are surface defects and hysteresis phenomena. Cao et al. [75] used pyrrolidine fullerene C_{60}-substituted phenol (NPC_{60}-OH) to weaken the hysteresis of SnO_2. The SnO_2/NPC_{60}-OH-based PSCs obtained a PCE of 21.39%. Liang et al. [76] passivated SnO_2 with chlorine to improve electron mobility. The open-circuit voltage increased from 1.195 V to

1.135 V. Jiang et al. [77] adopted phosphoric acid to increase the electron collection efficiency of SnO_2 by excluding its surface dangling bonds. Wang et al. [78] passivated SnO_2 ETLs by fullerene to improve the PCE and reproducibility. Cao et al. [79] modified the SnO_2 ETL by sulfur-doped graphite carbon nitride nanosheets to obtain a PCE of 20.33%. Liu et al. [80] introduced nontoxic phytic acid (PA) into the SnO_2 to obtain the ETL with fewer defects. PA-SnO_2-based PSCs had a high PCE of 21.43%. Lin et al. [81] obtained PCE of 21.87% with a SnO_2 ETL by precursor engineering. Li et al. [82] utilized vacuum-assisted annealing to synthesize a SnO_2 ETL at 100 °C for flexible solar cells, with a PCE of 20.14%. Liu et al. [83] adopted polydentate phytic acid dipotassium (PAD) to passivate the defects of the SnO_2/perovskite interface and obtained a PCE of 19.52%. Xu et al. introduced functional polymers such as polyethylene oxide-polypropylene oxide-polyethylene oxide (P123) [84] and poly(amidoamine) (PM) [85] in SnO_2 precursor to construct a uniform and dense SnO_2 ETL. The PM-treated PSC had a PCE of up to 22.93%, with negligible hysteresis. Zong et al. used continuous spin coating to fabricate SnO_2@K:Cs [86] and SnO_2@Na:Cs ETLs [87], respectively. The better PCE was 22.06%, based on a SnO_2@Na:Cs ETL. Gu et al. [88] added NaCl to raise the charge exchange between the SnO_2 ETL and perovskite and obtained a PCE of 21.2%. Large-scale fabrication methods include vacuum thermal evaporation [89], magnetron sputtering [90], radio frequency [91][92], sputtering deposition [93], spray deposition [94][95], atomic layer deposition [96], hydrothermal [97], and printing [98]. Doping can improve the properties of SnO_2. Common doping materials include Ga [99][100], Ta [101], Nb [102][103], Zn [104], Li [105], Zr/F [106], KF [107], Cl [108], NH_4Cl [109], and graphene quantum dots [110]. The performance of related PSCs is shown in **Table 1**. Double ELT is also a valid way to promote the performance of SnO_2, such as SnO_2/CdS [111], SnO_2-Ti_3C_2 Mxene [112], SnO_2/ZnO [113][114][115], SnO_2/TiO_2 [116][117], SnO_2/carbon nanotubes [118], SnO_2/KCl [119], SnO_2-assisted CdS [120], and NH_2-ZnO@SnO_2 [121].

ZnO, as another ETL material, has relatively large electron mobility, good light transmittance, proper work function, stability, low cost, and low-temperature preparation. Environmental friendliness, low-temperature, and large area are still hot topics of preparation method research. Zhang et al. [122] promoted the energy-level alignment and charge carrier extraction of ZnO by the sol–gel method. They also deposited ZnO by a simple water-based processing route [123]. Zhao et al. [124] used magnetron sputtering to prepare big-size grains, low defect state density, and a great optical ZnO ETL. They found that the PSCs based on an Ar/O_2 ratio of 1:4 treated ZnO had a maximum PCE of 17.22%. However, ZnO shows less chemical compatibility with the perovskite layer. Surface passivation and ion doping are frequently used strategies. Yang et al. [125] optimized the hydrophilicity of the ZnO surface with three amino compounds. They found that the PSCs with isobutylamine (IBA) modification exhibited improved stability, and PCE can reach 18.84%. Eswaramoorthy et al. [126] used plasmonic nanoparticles to modify ZnO for high PCE and stability. Commonly used doping materials are Al [127], Co [128], Mg [129][130], reduced graphene oxide (rGO) sheet/Ag [131], and PbS [132]. The performance of related PSCs is shown in **Table 1**.

Table 1. Summary of various PSCs performances using doped ETL.

ETL		Device Configuration	J_{sc} (mA cm^{-2})	V_{OC} (V)	FF	PCE (%)	Ref.
TiO_2	Li	FTO/c-TiO_2/Li-m-TiO_2/$MAPbI_3$/Spiro-	22.86	1.101	0.699	17.59	[44]

ETL		Device Configuration	J_{sc} (mA cm^{-2})	V_{OC} (V)	FF	PCE (%)	Ref.
		OMeTAD/Au					
	Mg	FTO/Mg-TiO_2/Perovskite/Spiro-OMeTAD/Au	22.27	1.08	0.609	14.65	[45]
	Zn	FTO/Zn-TiO_2/$MAPbI_3$/Spiro-OMeTAD/Au	21.83	1.10	0.734	17.60	[46]
	Zn	FTO/Zn-TiO_2 NAs/$(FAPbI_3)_{0.87}(MAPbBr_3)_{0.13}$/CuSCN/Carbon	22.25	0.956	0.679	14.45	[47]
	$EuAc_3$	FTO/$EuAc_3$-c-TiO_2/$CsPbI_3$/P3HT/Au	21.20	1.1	0.77	17.92	[48]
	Nb	FTO/Nb-TiO_2/$FA_{0.79}MA_{0.16}Cs_{0.05}Pb(Br_XI_{1-X})_3$/Spiro-OMeTAD/Au	24.70	1.12	0.78	21.30	[49]
	Ce	FTO/Ce-TiO_2/$MAPbI_3$/Spiro-OMeTAD/Ag	21.95	1.07	0.69	16.18	[51]
	Zr	FTO/Zr-TiO_2/$MAPbI_3$/Spiro-OMeTAD/Ag	23.66	0.92	0.567	12.35	[52]
	Zr	FTO/Zr-TiO_2/$MAPbI_3$/Spiro-OMeTAD/Au	23.57	1.076	0.716	18.16	[53]
	Ta	FTO/Ta-TiO_2/$Cs_{0.1}(FA_{0.83}MA_{0.17})_{0.9}Pb(I_{0.83}Br_{0.17})_3$/Spiro-OMeTAD/Ag	22.45	1.13	0.77	19.62	[54]
	GQDs	FTO/c-TiO_2/GQDs-mTiO_2/$Cs_{0.05}(FA_{0.83}MA_{0.17})_{0.95}$ $Pb(I_{0.83}Br_{0.17})_3$/Spiro-OMeTAD/Au	21.92	0.97	0.63	14.36	[56]
SnO_2	Ga	ITO/Ga-SnO_2/$(FAPbI_3)_x(MAPbBr_3)_{1-x}$/Spiro-OMeTAD/Ag	23.90	1.068	0.714	18.18	[99]
	Ga	FTO/Ga-SnO_x/$CsPbBr_3$/Carbon	7.58	1.311	0.602	5.98	[100]
	Ta	ITO/Ta-SnO_2/Perovskite/Spiro-OMeTAD/Au	22.79	1.161	0.786	20.8	[101]
	Nb	FTO/Nb-SnO_2/$CsPbBr_3$/Carbon	8.92	1.31	0.731	8.54	[103]
	Zn	FTO/Zn-SnO_2/$CsPbBr_3$/CuPc/Carbon	23.40	1.098	0.692	17.78	[104]
	Li	Li-FTO/SnO_2/Al_2O_3/$MAPbI_3$/Carbon	22.18	0.76	0.59	10.01	[105]
	Zr/F	FTO/Zr/F-SnO_2/Perovskite/Spiro-OMeTAD/Au	24.39	1.105	0.712	19.19	[106]
	KF	ITO/KF-SnO_2/$CsPbI_2Br$/Spiro-OMeTAD/MoO_3/Au	14.79	1.31	0.792	15.39	[107]
	Cl	FTO/Cl-SnO_2/Perovskite/Spiro-OMeTAD/Au	24.25	1.07	0.73	18.94	[108]

ETL		Device Configuration	J_{sc} (mA cm^{-2})	V_{OC} (V)	FF	PCE (%)	Ref.
ZnO	NH_4Cl	ITO/NH_4Cl-L-SnO_2/NH_4Cl-H-SnO_2/Perovskite/PEAI/Spiro-OMeTAD/Au	23.60	1.208	0.762	21.75	[109]
	GQDs	ITO/GQDs-SnO_2/$MAFAPbI_3Cl_{3-x}$/Spiro-OMeTAD/Ag	24.40	1.11	0.78	21.10	[110]
	Co	PET/ITO/Co-ZnO/$MAPbI_3$/Spiro-OMeTAD/Au	14.30	1.04	0.47	7.00	[128]
	Mg	FTO/Mg-ZnO/$MAPbI_3$/Spiro-OMeTAD/Ag	25.06	0.83	0.65	13.52	[130]
	rGO/Ag	FTO/rGO/Ag-ZnO/$MAPbI_3$/Spiro-OMeTAD/Au	17.82	0.90	0.72	11.03	[131]
	PbS	ITO/PbS-ZnO/$MAPbI_3$/Spiro-OMeTAD/Ag	22.8	1.14	0.79	20.53	[132]

1. Rab… Olabi, … 54,
3. Xu, L.; Yuan, S.; Ma, L.; Zhang, B.; Fang, T.; Li, X.; Song, J. All-inorganic perovskite quantum dots as light-harvesting, interfacial, and light-converting layers toward solar cells. J. Mater. Chem. A 2021, 9, 18947–18973.
4. Xiang, W.; Tress, W. Review on Recent Progress of All-Inorganic Metal Halide Perovskites and Solar Cells. Adv. Mater. 2019, 31, 1902851.
5. Wu, T.; Qin, Z.; Wang, Y.; Wu, Y.; Chen, W.; Zhang, S.; Cai, M.; Dai, S.; Zhang, J.; Liu, J.; et al. The Main Progress of Perovskite Solar Cells in 2020-2021. Nano-Micro Lett. 2021, 13, 152.
6. Wang, Z.; Zhang, Z.; Xie, L.; Wang, S.; Yang, C.; Fang, C.; Hao, F. Recent Advances and Perspectives of Photostability for Halide Perovskite Solar Cells. Adv. Opt. Mater. 2022, 10, 2101822.
7. Roy, P.; Ghosh, A.; Barclay, F.; Khare, A.; Cuce, E. Perovskite Solar Cells: A Review of the Recent Advances. Coatings 2022, 12, 1089.
8. Park, J.; Kim, J.; Yun, H.-S.; Paik, M.J.; Noh, E.; Mun, H.J.; Kim, M.G.; Shin, T.J.; Seok, S.I. Controlled growth of perovskite layers with volatile alkylammonium chlorides. Nature 2023.
9. Borriello, I.; Cantele, G.; Ninno, D. Ab initio investigation of hybrid organic-inorganic perovskites based on tin halides. Phys. Rev. B 2008, 77, 235214.
10. Li, H.; Zhang, W. Perovskite Tandem Solar Cells: From Fundamentals to Commercial Deployment. Chem. Rev. 2020, 120, 9835–9950.
11. Kieslich, G.; Sun, S.; Cheetham, A.K. Solid-state principles applied to organic–inorganic perovskites: New tricks for an old dog. Chem. Sci. 2014, 5, 4712–4715.
12. Kim, H.-S.; Im, S.H.; Park, N.-G. Organolead Halide Perovskite: New Horizons in Solar Cell Research. J. Phys. Chem. C 2014, 118, 5615–5625.
13. Pang, S.; Hu, H.; Zhang, J.; Lv, S.; Yu, Y.; Wei, F.; Qin, T.; Xu, H.; Liu, Z.; Cui, G. NH2CH=NH2PbI3: An Alternative Organolead Iodide Perovskite Sensitizer for Mesoscopic Solar

Cells. Chem. Mater. 2014, 26, 1485–1491.

14. Wang, Y.Q.; Fu, W.F.; Yan, J.L.; Chen, J.H.; Yang, W.T.; Chen, H.Z. Low-bandgap mixed tin-lead iodide perovskite with large grains for high performance solar cells. J. Mater. Chem. A 2018, 6, 13090–13095.
15. Li, Y.; Sun, W.; Yan, W.; Ye, S.; Rao, H.; Peng, H.; Zhao, Z.; Bian, Z.; Liu, Z.; Zhou, H.; et al. 50% Sn-Based Planar Perovskite Solar Cell with Power Conversion Efficiency up to 13.6%. Adv. Energy Mater. 2016, 6, 1601353.
16. Sahli, F.; Werner, J.; Kamino, B.A.; Braeuninger, M.; Monnard, R.; Paviet-Salomon, B.; Barraud, L.; Ding, L.; Leon, J.J.D.; Sacchetto, D.; et al. Fully textured monolithic perovskite/silicon tandem solar cells with 25.2% power conversion efficiency. Nat. Mater. 2018, 17, 820–826.
17. Jaysankar, M.; Filipic, M.; Zielinski, B.; Schmager, R.; Song, W.; Qiu, W.; Paetzold, U.W.; Aernouts, T.; Debucquoy, M.; Gehlhaar, R.; et al. Perovskite-silicon tandem solar modules with optimised light harvesting. Energy Environ. Sci. 2018, 11, 1489–1498.
18. Heo, J.H.; Im, S.H. CH3NH3PbBr3-CH3NH3PbI3 Perovskite-Perovskite Tandem Solar Cells with Exceeding 2.2 V Open Circuit Voltage. Adv. Mater. 2016, 28, 5121–5125.
19. Jost, M.; Kegelmann, L.; Korte, L.; Albrecht, S. Monolithic Perovskite Tandem Solar Cells: A Review of the Present Status and Advanced Characterization Methods Toward 30% Efficiency. Adv. Energy Mater. 2020, 10, 1904102.
20. Zhang, Y.; Gu, M.; Li, N.; Xu, Y.; Ling, X.; Wang, Y.; Zhou, S.; Li, F.; Yang, F.; Ji, K.; et al. Realizing solution-processed monolithic PbS QDs/perovskite tandem solar cells with high UV stability. J. Mater. Chem. A 2018, 6, 24693–24701.
21. Meng, L.; You, J.; Guo, T.-F.; Yang, Y. Recent Advances in the Inverted Planar Structure of Perovskite Solar Cells. Acc. Chem. Res. 2016, 49, 155–165.
22. Jeon, N.J.; Noh, J.H.; Kim, Y.C.; Yang, W.S.; Ryu, S.; Seok, S.I. Solvent engineering for high-performance inorganic-organic hybrid perovskite solar cells. Nat. Mater. 2014, 13, 897–903.
23. Jeon, N.J.; Na, H.; Jung, E.H.; Yang, T.-Y.; Lee, Y.G.; Kim, G.; Shin, H.-W.; Seok, S.I.; Lee, J.; Seo, J. A fluorene-terminated hole-transporting material for highly efficient and stable perovskite solar cells. Nat. Energy 2018, 3, 682–689.
24. Wu, W.-Q.; Chen, D.; Caruso, R.A.; Cheng, Y.-B. Recent progress in hybrid perovskite solar cells based on n-type materials. J. Mater. Chem. A 2017, 5, 10092–10109.
25. Kim, Y.S.; Jin, H.J.; Jung, H.R.; Kim, J.; Nguyen, B.P.; Kim, J.; Jo, W. Reduced extrinsic recombination process in anatase and rutile TiO2 epitaxial thin films for efficient electron transport layers. Sci. Rep. 2021, 11, 6810.

26. Maniarasu, S.; Karthikeyan, V.; Korukonda, T.B.; Pradhan, S.C.; Soman, S.; Ramasamy, E.; Veerappan, G. Ambient processed perovskite sensitized porous TiO2 nanorods for highly efficient and stable perovskite solar cells. J. Alloys Compod. 2021, 884, 161061.
27. Singh, M.; Chiang, C.-H.; Boopathi, K.M.; Hanmandlu, C.; Li, G.; Wu, C.-G.; Lin, H.-C.; Chu, C.-W. A novel ball milling technique for room temperature processing of TiO2 nanoparticles employed as the electron transport layer in perovskite solar cells and modules. J. Mater. Chem. A 2018, 6, 7114–7122.
28. Sun, J.; Pascoe, A.R.; Meyer, S.; Wu, Q.; Della Gaspera, E.; Raga, S.R.; Zhang, T.; Nattestad, A.; Bach, U.; Cheng, Y.-B.; et al. Ultrasonic spray deposition of TiO2 electron transport layers for reproducible and high efficiency hybrid perovskite solar cells. Sol. Energy 2019, 188, 697–705.
29. Lewis, A.; Troughton, J.R.; Smith, B.; McGettrick, J.; Dunlop, T.; De Rossi, F.; Pockett, A.; Spence, M.; Carnie, M.J.; Watson, T.M.; et al. In-depth analysis of defects in TiO2 compact electron transport layers and impact on performance and hysteresis of planar perovskite devices at low light. Sol. Energy Mater. Sol. Cells 2020, 209, 110448.
30. Chen, D.; Su, A.; Li, X.; Pang, S.; Zhu, W.; Xi, H.; Chang, J.; Zhang, J.; Zhang, C.; Hao, Y. Efficient planar perovskite solar cells with low-temperature atomic layer deposited TiO2 electron transport layer and interfacial modifier. Sol. Energy 2019, 188, 239–246.
31. Shahiduzzaman, M.; Sakuma, T.; Kaneko, T.; Tomita, K.; Isomura, M.; Taima, T.; Umezu, S.; Iwamori, S. Oblique Electrostatic Inkjet-Deposited TiO2 Electron Transport Layers for Efficient Planar Perovskite Solar Cells. Sci. Rep. 2019, 9, 19494.
32. Buffiere, M.; Ali, K.; Fares, E.; Samara, A.; Shetty, A.R.; Al Hassan, O.; Belaidi, A. Inkjet-Printed Compact TiO2 Electron Transport Layer for Perovskite Solar Cells. Energy Technol. 2020, 8, 2000330.
33. Huckaba, A.J.; Garcia-Benito, I.; Kanda, H.; Shibayama, N.; Oveisi, E.; Nazeeruddin, M.K. Inkjet-Printed TiO2/Fullerene Composite Films for Planar Perovskite Solar Cells. Helv. Chim. Acta 2020, 103, e2000044.
34. Liu, B.; Sun, G.; Sun, Q.; Lv, Y.; Huang, M.; Qi, B. Low-temperature fabrication of perovskite solar cells using modified TiO2 electron transport layer. Mater. Sci. Semicon. Proc. 2022, 138, 106303.
35. Noori, L.; Hoseinpour, V.; Shariatinia, Z. Optimization of TiO2 paste concentration employed as electron transport layers in fully ambient air processed perovskite solar cells with a low-cost architecture. Ceram. Int. 2022, 48, 320–336.
36. Supraja, S.; Dileep, K.R.; Chundi, N.; Ramasamy, E.; Shanmugasundaram, S.; Veerappan, G. Influence of bi-phasic TiO2 as a low-temperature curable electron transport layer for efficient perovskite solar cells. Sol. Energy 2022, 247, 308–314.

37. Ma, S.; Ahn, J.; Oh, Y.; Kwon, H.-C.; Lee, E.; Kim, K.; Yun, S.-C.; Moon, J. Facile Sol Gel-Derived Craterlike Dual-Functioning TiO2 Electron Transport Layer for High-Efficiency Perovskite Solar Cells. ACS Appl. Mater. Interfaces 2018, 10, 14649–14658.
38. Wang, K.; Zhao, W.; Li, H.; Li, D.; Liu, Z.; Wang, D.; Liu, S. Oxidation, reduction, and inert gases plasma-modified defects in TiO2 as electron transport layer for planar perovskite solar cells. J. CO2 Util. 2019, 32, 46–52.
39. Ranjan, S.; Ranjan, R.; Tyagi, A.; Rana, K.S.; Soni, A.; Kodali, H.K.; Dalal, V.; Singh, A.; Garg, A.; Nalwa, K.S.; et al. Low-Temperature Microwave Processed TiO2 as an Electron Transport Layer for Enhanced Performance and Atmospheric Stability in Planar Perovskite Solar Cells. ACS Appl. Energy Mater. 2022, 5, 2679–2696.
40. Wang, L.; Miao, Q.; Sun, Z.; Zhang, H.; Liu, Z.; Wang, G.; Zhang, S. In Situ Electron Transport Layers by a Carboxyl Ionic Liquid-Assisted Microwave Technique for a 20.1% Perovskite Solar Cell. ACS Appl. Energy Mater. 2021, 4, 12112–12120.
41. Jarwal, D.K.; Kumar, A.; Mishra, A.K.; Ratan, S.; Kumar, C.; Upadhyay, D.; Mukherjee, B.; Jit, S. Efficiency Improvement of TiO2 Nanorods Electron Transport Layer Based Perovskite Solar Cells by Solvothermal Etching. IEEE J. Photovolt. 2019, 9, 1699–1707.
42. Shahvaranfard, F.; Altomare, M.; Hou, Y.; Hejazi, S.; Meng, W.; Osuagwu, B.; Li, N.; Brabec, C.J.; Schmuki, P. Engineering of the Electron Transport Layer/Perovskite Interface in Solar Cells Designed on TiO2 Rutile Nanorods. Adv. Funct. Mater. 2020, 30, 1909738.
43. Lu, H.; Zhong, J.; Ji, C.; Zhao, J.; Li, D.; Zhao, R.; Jiang, Y.; Fang, S.; Liang, T.; Li, H.; et al. Fabricating an optimal rutile TiO2 electron transport layer by delicately tuning TiCl4 precursor solution for high performance perovskite solar cells. Nano Energy 2020, 68, 104336.
44. Amalathas, A.P.; Landova, L.; Conrad, B.; Holovsky, J. Concentration-Dependent Impact of Alkali Li Metal Doped Mesoporous TiO2 Electron Transport Layer on the Performance of CH3NH3PbI3 Perovskite Solar Cells. J. Phys. Chem. C 2019, 123, 19376–19384.
45. Arshad, Z.; Khoja, A.H.; Shakir, S.; Afzal, A.; Mujtaba, M.A.; Soudagar, M.E.M.; Fayaz, H.; Saleel, C.A.; Farukh, S.; Saeed, M. Magnesium doped TiO2 as an efficient electron transport layer in perovskite solar cells. Case Stud. Therm. Eng. 2021, 26, 101101.
46. Liu, X.; Wu, Z.; Zhang, Y.; Tsamis, C. Low temperature Zn-doped TiO2 as electron transport layer for 19% efficient planar perovskite solar cells. Appl. Surf. Sci. 2019, 471, 28–35.
47. Lv, Y.; Tong, H.; Cai, W.; Zhang, Z.; Chen, H.; Zhou, X. Boosting the efficiency of commercial available carbon-based perovskite solar cells using Zinc-doped TiO2 nanorod arrays as electron transport layer. J. Alloys Compod. 2021, 851, 156785.
48. Ren, W.; Liu, Y.; Wu, Y.; Sun, Q.; Cui, Y.; Hao, Y. Interface modification of an electron transport layer using europium acetate for enhancing the performance of P3HT-based inorganic perovskite

solar cells. Phys. Chem. Chem. Phys. 2021, 23, 23818–23826.

49. Sanehira, Y.; Shibayama, N.; Numata, Y.; Ikegami, M.; Miyasaka, T. Low-Temperature Synthesized Nb-Doped TiO2 Electron Transport Layer Enabling High-Efficiency Perovskite Solar Cells by Band Alignment Tuning. ACS Appl. Mater. Interfaces 2020, 12, 15175–15182.
50. Jin, J.; Li, H.; Bi, W.; Chen, C.; Zhang, B.; Xu, L.; Dong, B.; Song, H.; Dai, Q. Efficient and stable perovskite solar cells through e-beam preparation of cerium doped TiO2 electron transport layer, ultraviolet conversion layer CsPbBr3 and the encapsulation layer Al2O3. Sol. Energy 2020, 198, 187–193.
51. Xu, R.; Li, Y.; Feng, S.; Wang, J.; Zhang, J.; Zhang, X.; Bian, C.; Fu, W.; Li, Z.; Yang, H. Enhanced performance of planar perovskite solar cells using Ce-doped TiO2 as electron transport layer. J. Mater. Sci. 2020, 55, 5681–5689.
52. Qureshi, A.A.; Javed, H.M.A.; Javed, S.; Bashir, A.; Usman, M.; Akram, A.; Ahmad, M.I.; Ali, U.; Shahid, M.; Rizwan, M.; et al. Incorporation of Zr-doped TiO2 nanoparticles in electron transport layer for efficient planar perovskite solar cells. Surf. Interfaces 2021, 25, 101299.
53. Sandhu, S.; Saharan, C.; Buruga, S.K.; Kumar, S.A.; Rana, P.S.; Nagajyothi, P.C.; Mane, S.D. Micro structurally engineered hysteresis-free high efficiency perovskite solar cell using Zr-doped TiO2 electron transport layer. Ceram. Int. 2021, 47, 14665–14672.
54. Chen, K.-T.; Hsu, C.-H.; Jiang, S.-C.; Liang, L.-S.; Gao, P.; Qiu, Y.; Wu, W.-Y.; Zhang, S.; Zhu, W.-Z.; Lien, S.-Y. Effect of Annealing Temperature on Tantalum-Doped TiO2 as Electron Transport Layer in Perovskite Solar Cells. IEEE Trans. Electron Devices 2022, 69, 1149–1154.
55. Culu, A.; Kaya, I.C.; Sonmezoglu, S. Spray-Pyrolyzed Tantalium-Doped TiO2 Compact Electron Transport Layer for UV-Photostable Planar Perovskite Solar Cells Exceeding 20% Efficiency. ACS Appl. Energy Mater. 2022, 5, 3454–3462.
56. Ebrahimi, M.; Kermanpur, A.; Atapour, M.; Adhami, S.; Heidari, R.H.; Khorshidi, E.; Irannejad, N.; Rezaie, B. Performance enhancement of mesoscopic perovskite solar cells with GQDs-doped TiO2 electron transport layer. Sol. Energy Mater. Sol. Cells 2020, 208, 110407.
57. Liu, Z.; Sun, B.; Liu, X.; Han, J.; Ye, H.; Tu, Y.; Chen, C.; Shi, T.; Tang, Z.; Liao, G. 15% efficient carbon based planar-heterojunction perovskite solar cells using a TiO2/SnO2 bilayer as the electron transport layer. J. Mater. Chem. A 2018, 6, 7409–7419.
58. Mali, S.S.; Patil, J.V.; Arandiyan, H.; Hong, C.K. Reduced methylammonium triple-cation Rb0.05(FAPbI3)0.95(MAPbBr3)0.05 perovskite solar cells based on a TiO2/SnO2 bilayer electron transport layer approaching a stabilized 21% efficiency: The role of antisolvents. J. Mater. Chem. A 2019, 7, 17516–17528.
59. Xie, H.; Yin, X.; Liu, J.; Guo, Y.; Chen, P.; Que, W.; Wang, G.; Gao, B. Low temperature solution-derived TiO2-SnO2 bilayered electron transport layer for high performance perovskite solar cells.

Appl. Surf. Sci. 2019, 464, 700–707.

60. Mohammadbeigi, A.; Mozaffari, S.; Ghorashi, S.M.B. Yolk-shell SnO2@TiO2 nanospheres as electron transport layer in mesoscopic perovskite solar cell. J. Sol-Gel Sci. Technol. 2020, 94, 731–742.
61. Li, N.; Yan, J.; Ai, Y.; Jiang, E.; Lin, L.; Shou, C.; Yan, B.; Sheng, J.; Ye, J. A low-temperature TiO2/SnO2 electron transport layer for high-performance planar perovskite solar cells. Sci. China Mater. 2020, 63, 207–215.
62. Chiang, C.H.; Kan, C.W.; Wu, C.G. Synergistic Engineering of Conduction Band, Conductivity, and Interface of Bilayered Electron Transport Layers with Scalable TiO2 and SnO2 Nanoparticles for High-Efficiency Stable Perovskite Solar Cells. ACS Appl. Mater. Interfaces 2021, 13, 23606–23615.
63. Koech, R.K.; Ichwani, R.; Oyewole, D.; Kigozi, M.; Amune, D.; Sanni, D.M.; Adeniji, S.; Oyewole, K.; Bello, A.; Ntsoenzok, E.; et al. Tin Oxide Modified Titanium Dioxide as Electron Transport Layer in Formamidinium-Rich Perovskite Solar Cells. Energies 2021, 14, 7870.
64. Ko, Y.; Kim, T.; Lee, C.; Lee, C.; Yun, Y.J.; Jun, Y. Alleviating Interfacial Recombination of Heterojunction Electron Transport Layer via Oxygen Vacancy Engineering for Efficient Perovskite Solar Cells Over 23%. Energy Environ. Mater. 2022, 0, 1–12.
65. Paik, M.J.; Yoo, J.W.; Park, J.; Noh, E.; Kim, H.; Ji, S.-G.; Kim, Y.Y.; Il Seok, S. SnO2-TiO2 Hybrid Electron Transport Layer for Efficient and Flexible Perovskite Solar Cells. ACS Energy Lett. 2022, 7, 1864–1870.
66. Zhou, J.; Lyu, M.; Zhu, J.; Li, G.; Li, Y.; Jin, S.; Song, J.; Niu, H.; Xu, J.; Zhou, R. SnO2 Quantum Dot-Modified Mesoporous TiO2 Electron Transport Layer for Efficient and Stable Perovskite Solar Cells. ACS Appl. Energy Mater. 2022, 5, 3052–3063.
67. Wang, D.; Ni, J.; Guan, J.; Zhou, X.; Zhang, S.; Zhang, Y.; Huang, Q.; Cai, H.; Li, J.; Zhang, J. Thin Film of TiO2-ZnO Binary Mixed Nanoparticles as Electron Transport Layers in Low-Temperature Processed Perovskite Solar Cells. Nano 2020, 15, 2050036.
68. Yue, M.; Su, J.; Zhao, P.; Lin, Z.H.; Zhang, J.C.; Chang, J.J.; Hao, Y. Optimizing the Performance of CsPbI3-Based Perovskite Solar Cells via Doping a ZnO Electron Transport Layer Coupled with Interface Engineering. Nano-Micro Lett. 2019, 11, 91.
69. Wang, F.Y.; Yang, M.F.; Zhang, Y.H.; Du, J.Y.; Han, D.L.; Yang, L.L.; Fan, L.; Sui, Y.R.; Sun, Y.F.; Meng, X.W.; et al. Constructing m-TiO2/a-WOx hybrid electron transport layer to boost interfacial charge transfer for efficient perovskite solar cells. Chem. Eng. J. 2020, 402, 126303.
70. You, Y.; Tian, W.; Min, L.; Cao, F.; Deng, K.; Li, L. TiO2/WO3 Bilayer as Electron Transport Layer for Efficient Planar Perovskite Solar Cell with Efficiency Exceeding 20%. Adv. Mater. Interfaces 2020, 7, 1901406.

71. Dadashbeik, M.; Fathi, D.; Eskandari, M. Design and simulation of perovskite solar cells based on graphene and TiO2/graphene nanocomposite as electron transport layer. Sol. Energy 2020, 207, 917–924.
72. Mohseni, H.R.; Dehghanipour, M.; Dehghan, N.; Tamaddon, F.; Ahmadi, M.; Sabet, M.; Behjat, A. Enhancement of the photovoltaic performance and the stability of perovskite solar cells via the modification of electron transport layers with reduced graphene oxide/polyaniline composite. Sol. Energy 2021, 213, 59–66.
73. Zhao, Y.; Zhang, H.; Ren, X.G.; Zhu, H.L.; Huang, Z.F.; Ye, F.; Ouyang, D.; Cheah, K.W.; Jen, A.K.Y.; Choy, W.C.H. Thick TiO2-Based Top Electron Transport Layer on Perovskite for Highly Efficient and Stable Solar Cells. ACS Energy Lett. 2018, 3, 2891–2898.
74. Zhang, X.; Zhang, W.; Wu, T.; Wu, J.; Lan, Z. High efficiency and negligible hysteresis planar perovskite solar cells based on NiO nanocrystals modified TiO2 electron transport layers. Sol. Energy 2019, 181, 293–300.
75. Cao, T.; Chen, K.; Chen, Q.; Zhou, Y.; Chen, N.; Li, Y. Fullerene Derivative-Modified SnO2 Electron Transport Layer for Highly Efficient Perovskite Solar Cells with Efficiency over 21%. ACS Appl. Mater. Interfaces 2019, 11, 33825–33834.
76. Liang, J.; Chen, Z.; Yang, G.; Wang, H.; Ye, F.; Tao, C.; Fang, G. Achieving High Open-Circuit Voltage on Planar Perovskite Solar Cells via Chlorine-Doped Tin Oxide Electron Transport Layers. ACS Appl. Mater. Interfaces 2019, 11, 23152–23159.
77. Jiang, E.; Ai, Y.; Yan, J.; Li, N.; Lin, L.; Wang, Z.; Shou, C.; Yan, B.; Zeng, Y.; Sheng, J.; et al. Phosphate-Passivated SnO2 Electron Transport Layer for High-Performance Perovskite Solar Cells. ACS Appl. Mater. Interfaces 2019, 11, 36727–36734.
78. Wang, J.; Datta, K.; Weijtens, C.H.L.; Wienk, M.M.; Janssen, R.A.J. Insights into Fullerene Passivation of SnO2 Electron Transport Layers in Perovskite Solar Cells. Adv. Funct. Mater. 2019, 29, 1905883.
79. Cao, W.; Zhang, J.; Lin, K.; Qiu, L.; Li, J.; Dong, Y.; Wang, J.; Xia, D.; Fan, R.; Yang, Y. Enhanced Charge Transport and Interface Passivation in Efficient Perovskite Solar Cells Using Sulfur-Doped Graphite Carbon Nitride-Modified SnO2-Based Electron Transport Layers. Sol. RRL 2021, 5, 2100058.
80. Liu, C.; Su, H.; Xie, K.; Wang, H.; Zhai, P.; Chang, N.; Zhang, S.; Ban, Q.; Guo, M.; Zhang, J.; et al. Highly Enhanced Efficiency of Planar Perovskite Solar Cells by an Electron Transport Layer Using Phytic Acid-Complexed SnO2 Colloids. Sol. RRL 2021, 5, 2100067.
81. Lin, Z.C.; Zhang, W.Q.; Cai, Q.B.; Xu, X.N.; Dong, H.Y.; Mu, C.; Zhang, J.P. Precursor Engineering of the Electron Transport Layer for Application in High-Performance Perovskite Solar Cells. Adv. Sci. 2021, 8, 2102845.

82. Li, X.; Shi, Z.; Behrouznejad, F.; Hatamvand, M.; Zhang, X.; Wang, Y.; Liu, F.; Wang, H.; Liu, K.; Dong, H.; et al. Highly efficient flexible perovskite solar cells with vacuum-assisted low-temperature annealed SnO2 electron transport layer. J. Energy Chem. 2022, 67, 1–7.
83. Liu, C.; Guo, M.; Su, H.; Zhai, P.; Xie, K.; Liu, Z.; Zhang, J.; Liu, L.; Fu, H. Highly improved efficiency and stability of planar perovskite solar cells via bifunctional phytic acid dipotassium anchored SnO2 electron transport layer. Appl. Surf. Sci. 2022, 588, 152943.
84. Xu, Z.; Zhou, X.; Li, X.; Zhang, P. Polymer-Regulated SnO2 Composites Electron Transport Layer for High-Efficiency n-i-p Perovskite Solar Cells. Sol. RRL 2022, 6, 2200092.
85. Xu, Z.; Ng, C.H.; Zhou, X.; Li, X.; Zhang, P.; Teo, S.H. Polymer-complexed SnO2 electron transport layer for high-efficiency n-i-p perovskite solar cells. Nanoscale 2022, 14, 12090–12098.
86. Zong, B.; Deng, J.; Sun, Q.; Zhang, Z.; Meng, X.; Shen, B.; Kang, B.; Silva, S.R.P.; Lu, G. Facile Surface Engineering of Composite Electron Transport Layer for Highly Efficient Perovskite Solar Cells with a Fill Factor Exceeding 81%. Adv. Mater. Interfaces 2022, 9, 2102331.
87. Zong, B.; Sun, Q.; Deng, J.; Meng, X.; Zhang, Z.; Kang, B.; Silva, S.R.P.; Lu, G. Multi-cation hybrid stannic oxide electron transport layer for high-efficiency perovskite solar cells. J. Colloid Interface Sci. 2022, 614, 415–424.
88. Gu, L.; Wang, C.; Mo, W.; Zeng, H.; Shou, C.; Yang, S.; Wen, F. High efficiency perovskite solar cells via NaCl modified tin oxide electron transport layer. Org. Electron. 2023, 113, 106677.
89. Guo, Y.; Yin, X.; Liu, J.; Chen, W.; Wen, S.; Que, M.; Xie, H.; Yang, Y.; Que, W.; Gao, B. Vacuum thermal-evaporated SnO2 as uniform electron transport layer and novel management of perovskite intermediates for efficient and stable planar perovskite solar cells. Org. Electron. 2019, 65, 207–214.
90. Bai, G.; Wu, Z.; Li, J.; Bu, T.; Li, W.; Li, W.; Huang, F.; Zhang, Q.; Cheng, Y.-B.; Zhong, J. High performance perovskite sub-module with sputtered SnO2 electron transport layer. Sol. Energy 2019, 183, 306–314.
91. Kam, M.; Zhu, Y.; Zhang, D.; Gu, L.; Chen, J.; Fan, Z. Efficient Mixed-Cation Mixed-Halide Perovskite Solar Cells by All-Vacuum Sequential Deposition Using Metal Oxide Electron Transport Layer. Sol. RRL 2019, 3, 1900050.
92. Kam, M.; Zhang, Q.P.; Zhang, D.Q.; Fan, Z.Y. Room-Temperature Sputtered SnO2 as Robust Electron Transport Layer for Air-Stable and Efficient Perovskite Solar Cells on Rigid and Flexible Substrates. Sci. Rep. 2019, 9, 6963.
93. Qiu, L.; Liu, Z.; Ono, L.K.; Jiang, Y.; Son, D.-Y.; Hawash, Z.; He, S.; Qi, Y. Scalable Fabrication of Stable High Efficiency Perovskite Solar Cells and Modules Utilizing Room Temperature Sputtered SnO2 Electron Transport Layer. Adv. Funct. Mater. 2019, 29, 1806779.

94. Guan, J.; Ni, J.; Zhou, X.; Liu, Y.; Yin, J.; Wang, J.; Wang, D.; Zhang, Y.; Li, J.; Cai, H.; et al. High-Performance Electron Transport Layer via Ultrasonic Spray Deposition for Commercialized Perovskite Solar Cells. ACS Appl. Energy Mater. 2020, 3, 11570–11580.
95. Kumar, N.; Lee, H.B.; Sahani, R.; Tyagi, B.; Cho, S.; Lee, J.-S.; Kang, J.-W. Room-Temperature Spray Deposition of Large-Area SnO2 Electron Transport Layer for High Performance, Stable FAPbI(3)-Based Perovskite Solar Cells. Small Methods 2022, 6, 2101127.
96. Erdenebileg, E.; Wang, H.; Li, J.; Singh, N.; Dewi, H.A.; Tiwari, N.; Mathews, N.; Mhaisalkar, S.; Bruno, A. Low-Temperature Atomic Layer Deposited Electron Transport Layers for Co-Evaporated Perovskite Solar Cells. Sol. RRL 2022, 6, 2100842.
97. Liu, C.; Zhang, L.; Zhou, X.; Gao, J.; Chen, W.; Wang, X.; Xu, B. Hydrothermally Treated SnO2 as the Electron Transport Layer in High-Efficiency Flexible Perovskite Solar Cells with a Certificated Efficiency of 17.3%. Adv. Funct. Mater. 2019, 29, 1807604.
98. Liu, J.; Li, S.; Liu, S.; Chu, Y.; Ye, T.; Qiu, C.; Qiu, Z.; Wang, X.; Wang, Y.; Su, Y.; et al. Oxygen Vacancy Management for High-Temperature Mesoporous SnO2 Electron Transport Layers in Printable Perovskite Solar Cells. Angew. Chem. Int. Ed. 2022, 61, e202202012.
99. Ma, Z.; Zhou, W.; Xiao, Z.; Zhang, H.; Li, Z.; Zhuang, J.; Pen, C.; Huang, Y. Negligible hysteresis planar perovskite solar cells using Ga-doped SnO2 nanocrystal as electron transport layers. Org. Electron. 2019, 71, 98–105.
100. Zhao, Y.; Deng, Q.; Guo, R.; Wu, Z.; Li, Y.; Duan, Y.; Shen, Y.; Zhang, W.; Shao, G. Sputtered Ga-Doped SnOx Electron Transport Layer for Large-Area All-Inorganic Perovskite Solar Cells. ACS Appl. Mater. Interfaces 2020, 12, 54904–54915.
101. Liu, Q.; Zhang, X.; Li, C.; Lu, H.; Weng, Z.; Pan, Y.; Chen, W.; Hang, X.-C.; Sun, Z.; Zhan, Y. Effect of tantalum doping on SnO2 electron transport layer via low temperature process for perovskite solar cells. Appl. Phys. Lett. 2019, 115, 143903.
102. Song, J.; Xu, X.; Wu, J.; Lan, Z. Low-temperature solution-processing high quality Nb-doped SnO2 nanocrystals-based electron transport layers for efficient planar perovskite solar cells. Funct. Mater. Lett. 2019, 12, 1850091.
103. Guo, R.X.; Zhao, Y.; Zhang, Y.S.; Deng, Q.R.; Shen, Y.L.; Zhang, W.; Shao, G.S. Significant performance enhancement of all-inorganic CsPbBr3 perovskite solar cells enabled by Nb-doped SnO2 as effective electron transport layer. Energy Environ. Mater. 2021, 4, 671–680.
104. Ye, H.; Liu, Z.; Liu, X.; Sun, B.; Tan, X.; Tu, Y.; Shi, T.; Tang, Z.; Liao, G. 17.78% efficient low-temperature carbon-based planar perovskite solar cells using Zn-doped SnO2 electron transport layer. Appl. Surf. Sci. 2019, 478, 417–425.
105. Qiang, Y.; Xie, Y.; Qi, Y.; Wei, P.; Shi, H.; Geng, C.; Liu, H. Enhanced performance of carbon-based perovskite solar cells with a Li+-doped SnO2 electron transport layer and Al2O3 scaffold

layer. Sol. Energy 2020, 201, 523–529.

106. Tian, J.; Zhang, J.; Li, X.; Cheng, B.; Yu, J.; Ho, W. Low-Temperature-Processed Zr/F Co-Doped SnO2 Electron Transport Layer for High-Efficiency Planar Perovskite Solar Cells. Sol. RRL 2020, 4, 2000090.
107. Zhang, S.; Gu, H.; Chen, S.-C.; Zheng, Q. KF-Doped SnO2 as an electron transport layer for efficient inorganic CsPbI2Br perovskite solar cells with enhanced open-circuit voltages. J. Mater. Chem. C 2021, 9, 4240–4247.
108. Wu, J.-B.; Zhen, C.; Liu, G. Photo-assisted Cl doping of SnO2 electron transport layer for hysteresis-less perovskite solar cells with enhanced efficiency. Rare Met. 2022, 41, 361–367.
109. Ye, J.; Li, Y.; Medjahed, A.A.; Pouget, S.; Aldakov, D.; Liu, Y.; Reiss, P. Doped Bilayer Tin(IV) Oxide Electron Transport Layer for High Open-Circuit Voltage Planar Perovskite Solar Cells with Reduced Hysteresis. Small 2021, 17, 2005671.
110. Pang, S.; Zhang, C.; Zhang, H.; Dong, H.; Chen, D.; Zhu, W.; Xi, H.; Chang, J.; Lin, Z.; Zhang, J.; et al. Boosting performance of perovskite solar cells with Graphene quantum dots decorated SnO2 electron transport layers. Appl. Surf. Sci. 2020, 507, 145099.
111. Mohamadkhani, F.; Javadpour, S.; Taghavinia, N. Improvement of planar perovskite solar cells by using solution processed SnO2/CdS as electron transport layer. Sol. Energy 2019, 191, 647–653.
112. Yang, L.; Dall'Agnese, Y.; Hantanasirisakul, K.; Shuck, C.E.; Maleski, K.; Alhabeb, M.; Chen, G.; Gao, Y.; Sanehira, Y.; Jena, A.K.; et al. SnO2-Ti3C2 MXene electron transport layers for perovskite solar cells. J. Mater. Chem. A 2019, 7, 5635–5642.
113. Noh, Y.W.; Jin, I.S.; Kim, K.S.; Park, S.H.; Jung, J.W. Reduced energy loss in SnO2/ZnO bilayer electron transport layer-based perovskite solar cells for achieving high efficiencies in outdoor/indoor environments. J. Mater. Chem. A 2020, 8, 17163–17173.
114. Khan, U.; Iqbal, T.; Khan, M.; Wu, R. SnO2/ZnO as double electron transport layer for halide perovskite solar cells. Sol. Energy 2021, 223, 346–350.
115. He, R.Q.; Nie, S.Q.; Huang, X.F.; Wu, Y.Z.; Chen, R.H.; Yin, J.; Wu, B.H.; Li, J.; Zheng, N.F. Scalable Preparation of High-Performance ZnO-SnO2 Cascaded Electron Transport Layer for Efficient Perovskite Solar Modules. Sol. RRL 2022, 6, 2100639.
116. Luo, X.; Gao, Y.; Zhu, P.; Han, Q.; Lin, R.; Gao, H.; Wang, Y.; Zhu, J.; Li, S.; Tan, H. Record Photocurrent Density over 26 mA cm(-2) in Planar Perovskite Solar Cells Enabled by Antireflective Cascaded Electron Transport Layer. Sol. RRL 2020, 4, 2000169.
117. Liu, B.-T.; Zhang, Y.-Z.; Zuo, Y.-Y.; Rachmawati, D. Passivation and energy-level change of the SnO2 electron transport layer by reactive titania for perovskite solar cells. J. Alloys Compod. 2022, 929, 167349.

118. Tang, H.; Cao, Q.; He, Z.; Wang, S.; Han, J.; Li, T.; Gao, B.; Yang, J.; Deng, D.; Li, X. SnO2-Carbon Nanotubes Hybrid Electron Transport Layer for Efficient and Hysteresis-Free Planar Perovskite Solar Cells. Sol. RRL 2020, 4, 1900415.
119. Zhu, P.; Gu, S.; Luo, X.; Gao, Y.; Li, S.; Zhu, J.; Tan, H. Simultaneous Contact and Grain-Boundary Passivation in Planar Perovskite Solar Cells Using SnO2-KCl Composite Electron Transport Layer. Adv. Energy Mater. 2020, 10, 1903083.
120. Zhou, J.; Zhou, R.; Zhu, J.; Jiang, P.; Wan, L.; Niu, H.; Hu, L.; Yang, X.; Xu, J.; Xu, B. Colloidal SnO2-Assisted CdS Electron Transport Layer Enables Efficient Electron Extraction for Planar Perovskite Solar Cells. Sol. RRL 2021, 5, 2100494.
121. Zhao, R.; Wang, L.; Huang, J.; Miao, X.; Sun, L.; Hua, Y.; Wang, Y. Amino-capped zinc oxide modified tin oxide electron transport layer for efficient perovskite solar cells. Cell Rep. Phys. Sci. 2021, 2, 100590.
122. Zhang, J.; Tan, C.H.; Du, T.; Morbidoni, M.; Lin, C.-T.; Xu, S.; Durrant, J.R.; McLachlan, M.A. ZnO-PCBM bilayers as electron transport layers in low-temperature processed perovskite solar cells. Sci. Bull. 2018, 63, 343–348.
123. Zhang, J.; Morbidoni, M.; Huang, K.; Feng, S.; McLachlan, M.A. Environmentally friendly, aqueous processed ZnO as an efficient electron transport layer for low temperature processed metal-halide perovskite photovoltaics. Inorg. Chem. Front. 2018, 5, 84–89.
124. Zhao, W.; Li, H.; Li, D.; Liu, Z.; Wang, D.; Liu, S. Comprehensive investigation of sputtered and spin-coated zinc oxide electron transport layers for highly efficient and stable planar perovskite solar cells. J. Power Sources 2019, 427, 223–230.
125. Yang, Z.; Fan, Q.; Shen, T.; Jin, J.; Deng, W.; Xin, J.; Huang, X.; Wang, X.; Li, J. Amine-passivated ZnO electron transport layer for thermal stability-enhanced perovskite solar cells. Sol. Energy 2020, 204, 223–230.
126. Eswaramoorthy, N.; Rajaram, K. Planar perovskite solar cells: Plasmonic nanoparticles-modified ZnO as an electron transport layer for enhancing the device performance and stability at ambient conditions. Int. J. Energy Res. 2022, 46, 10724–10740.
127. Adnan, M.; Usman, M.; Ali, S.; Javed, S.; Islam, M.; Akram, M.A. Aluminum Doping Effects on Interface Depletion Width of Low Temperature Processed ZnO Electron Transport Layer-Based Perovskite Solar Cells. Front. Chem. 2022, 9, 795291.
128. Bouhjar, F.; Derbali, L.; Mari, B. High performance novel flexible perovskite solar cell based on a low-cost-processed ZnO:Co electron transport layer. Nano Res. 2020, 13, 2546–2555.
129. Ierides, I.; Ligorio, G.; McLachlan, M.A.; Guo, K.; List-Kratochvil, E.J.W.; Cacialli, F. Inverted organic photovoltaics with a solution-processed Mg-doped ZnO electron transport layer annealed at 150 degrees C. Sustain. Energy Fuels 2022, 6, 2835–2845.

130. Arshad, Z.; Wageh, S.; Maiyalagan, T.; Ali, M.; Arshad, U.; Noor ul, a.; Qadir, M.B.; Mateen, F.; Al-Sehemi, A.G. Enhanced charge transport characteristics in zinc oxide nanofibers via Mg2+ doping for electron transport layer in perovskite solar cells and antibacterial textiles. Ceram. Int. 2022, 48, 24363–24371.

131. Bagha, G.; Mersagh, M.R.; Naffakh-Moosavy, H.; Matin, L.F. The role of rGO sheet and Ag dopant in reducing ZnO electron transport layer recombination in planar perovskite solar cells. Ceram. Int. 2021, 47, 16111–16123.

132. Pang, Z.; Yang, S.; Sun, Y.; He, L.; Wang, F.; Fan, L.; Chi, S.; Sun, X.; Yang, L.; Yang, J. Hydrophobic PbS QDs layer decorated ZnO electron transport layer to boost photovoltaic performance of perovskite solar cells. Chem. Eng. J. 2022, 439, 135701.